


Spectroscopic and Imaging Characteristics of Pigmented Non-Melanoma Skin Cancer and Melanoma in Patients with Skin Phototypes III and IV

Stefanie Arroyo-Camarena  · Judith Domínguez-Cherit · Lorena Lammoglia-Ordiales ·

Diego A. Fabila-Bustos · Abraham Escobar-Pio · Suren Stolik ·

Alma Valor-Reed · José de la Rosa-Vázquez

Received: August 5, 2016 / Published online: December 12, 2016

© The Author(s) 2016. This article is published with open access at Springerlink.com

ABSTRACT

Introduction: Non-melanoma skin cancer is the most common malignancy worldwide. Differentiating between malignant and benign skin tumors, however, can be challenging. As a result, various auxiliary tools have been developed to aid in the diagnosis of cutaneous neoplasms. Here, skin tumors were investigated

Enhanced Content To view enhanced content for this article go to <http://www.medengine.com/Redeem/4627F0603B3AA17A>.

S. Arroyo-Camarena (✉) · L. Lammoglia-Ordiales
División de Dermatología, Hospital General
“Dr. Manuel Gea González”, 14080 Ciudad de
México, México
e-mail: dra.arroyocamarena@gmail.com

J. Domínguez-Cherit
Departamento de Dermatología, Instituto Nacional
de Ciencias Médicas y Nutrición “Salvador Zubirán”,
14080 Ciudad de México, México

D. A. Fabila-Bustos · A. Escobar-Pio · S. Stolik ·
A. Valor-Reed · J. de la Rosa-Vázquez
Laboratorio de Biofotónica, ESIME Zac, Instituto
Politécnico Nacional, 07738 Ciudad de México,
México

D. A. Fabila-Bustos
Departamento de Formación Básica Disciplinaria,
UPIIH, Instituto Politécnico Nacional, Ciudad del
Conocimiento y la Cultura, 42162 Pachuca de Soto,
Hidalgo, México

through analysis of their digital image histograms and spectroscopic response under ultraviolet (UV) and white light-emitting diodes (LEDs).

Methods: Fifty tumoral lesions were spectroscopically and histologically studied. For optical studies, UV at 375 nm and white LEDs were used to illuminate the lesions. Commercial cameras were used for imaging, and a miniature spectrometer with a bifurcated optical fiber was used for spectroscopic measurements.

Results: In this study, the intensity histograms of the images taken under white and UV illumination and the spectroscopic response under white light showed clear differences between pigmented basal cell carcinoma (BCC), intradermal melanocytic nevus (IDN), and melanoma lesions for skin phototypes III and IV. However, there was little difference in their spectroscopic response to the UV LED.

Conclusion: We found differences in the intensity and shape of diffuse reflectance spectra of pigmented BCC, IDN, and melanoma lesions in patients with skin phototypes III and IV. Also, images taken under UV and white light were helpful for differentiation of these pigmented lesions. Additional research is

needed to ascertain the clinical utility of these tools for skin cancer diagnosis.

Keywords: Digital images; Melanoma; Skin cancer; Spectroscopy

INTRODUCTION

Skin cancer is the most common malignancy worldwide [1], and can be classified into two groups: non-melanoma skin cancer (NMSC) and melanoma. Of the former, 95% of cases are basal cell carcinoma (BCC) or squamous cell carcinoma (SCC), although other, rare malignant skin tumors also belong to the NMSC classification [2].

Non-melanoma skin cancer is the most common type of cancer in white populations [3]. In Mexico, the incidence of NMSC is thought to be underreported, as it ranks third in overall incidence, after lung and cervical cancer, according to a 2008 report by the National Cancer Institute. Skin cancer ranks first in consultations among men and fourth among women [4].

In BCC, the affected skin areas are primarily those that are exposed. Though it progresses slowly, BCC is locally aggressive and destructive; however, metastasis is rare (only 0.05% of cases) [5]. The SCC type is most common on the face and lower extremities, and the risk of metastasis is ~5% [6]. In a study of clinical–pathological concordance conducted in our department, SCC and BCC were found to be the cancers most frequently confused with one another [7].

Melanoma, on the other hand, has seen the greatest increase per year worldwide [8]. In Mexico, it is estimated to occur at a rate of 1 in 100,000, but the actual figure is likely higher due to underreporting [9]. Although

superficially spreading melanoma is the most common subtype in whites [8], a study performed in the Hospital General Manuel Gea González in Mexico City found that acral lentiginous melanoma was the most frequent subtype in the studied population [9].

The differential diagnosis of skin cancer includes common benign neoplasms such as seborrheic keratosis (SK) [10] and melanocytic nevi. Precursor lesions, such as actinic keratosis (AK) [11], are also a differential diagnosis of SCC in situ, and in some studies even represent an emerging SCC [3]. Pigmented epidermal tumors can also be confused with lentigo maligna.

There are several auxiliary noninvasive methods for the clinical diagnosis of skin cancer. One such method is dermoscopy, which increases diagnostic accuracy from 5 to 30% over visual inspection; nonetheless, it requires expert evaluation [12, 13]. Finally, histopathology is the gold standard for diagnosis, but it is an invasive method.

In efforts to improve diagnosis, many new devices and tools have been developed, including reflectance confocal microscopy (RCM), and fluorescence, Raman, and reflectance spectroscopy, with promising results [14–16]. Specifically, RCM is a noninvasive method for real-time evaluation of skin lesions, similar to histological images [15]. However, this technique requires special training and is expensive [17]. Diffuse reflectance spectroscopy and fluorescence spectroscopy operate based on light–matter interaction, and both are promising noninvasive tools for the diagnosis of cancer [18, 19]. Their basic premise is that the emission and scattering of light depends on the composition and cell structure of tissues. Skin lesions cause a change in composition and cell structure, and thus produce a change in light scattering as well as in fluorescence emission.

Various investigations of biological tissue have reported the use of diffuse reflectance and fluorescence spectroscopy [20–23]. Pilot studies have shown that fluorescence intensity is greater at higher concentrations of skin melanin. Furthermore, spectral distribution patterns have been found to vary for different types of skin lesions [24]. In addition, capturing images of skin lesions using UV fluorescence can reveal relevant information not easily obtained under white light [25].

The purpose of this study was to take advantage of the fluorescence and diffuse reflectance of the skin tissue as reflected in the red, green, and blue (RGB) histograms of images obtained by a digital camera. This study can thus shed light on the utility of these techniques as noninvasive diagnostic aids in NMSC and melanoma, and their primary differential diagnoses.

METHODS

Our potential sample included patients from the dermatology outpatient department at the General Hospital “Dr. Manuel Gea González” in Mexico City, who received a diagnosis of skin cancer or other benign skin tumors, and were scheduled for an incisional or excisional biopsy during the period between October 2013 and April 2014. Patients who signed the informed consent form and attended the spectroscopy measurement and lesion photography sessions were included in the study. Patients who had no histopathological results were excluded from the sample, as were those who did not sign the informed consent form.

The equipment used in this study included a Sony Cyber-shot DSC-HX200V digital camera with a CMOS sensor, 18.2 million effective pixels in each picture, and a 30× optical

zoom. The images were stored on a secure digital (SD) memory card and were later downloaded to a computer for processing. In addition, a Nikon® D5100 camera was used for taking digital images. This camera has CMOS sensors, with a resolution of 16.2 megapixels and 3× optical zoom. An SD card was likewise used for image storage.

For spectroscopic measurements, a miniature spectrometer USB4000-VIS-IR and a bifurcated optical fiber QR400-7-UV/VIS (both Ocean Optics, Inc., Dunedin, FL, USA) were used. In addition, a laptop with National Instruments LabVIEW 2010 software installed was used to save the data.

For spectroscopic measurements and imaging, light-emitting diodes (LEDs) were used. These included LEDs emitting white light in a range of 450–750 nm (LED-P3 W200-120/41SiLed Int.) and an LED emitting ultraviolet light at a nominal wavelength of 365 nm, with 20-nm full width at half maximum (FWHM) bandwidth (NCU033AT, Nichia Corp.). An appropriate current source was designed and built to feed the LEDs, which yielded maximum radiation intensity of 1.6 and 1 W for white and UV light, respectively. For imaging under white light, two illumination panels of ten white LEDs each were mounted and used to homogeneously illuminate the lesion to be photographed, placing the panels in a vertical position at a maximum distance of 50 cm from the studied area. The photographs under UV light were taken using one UV LED located 20 cm from the lesion. In all cases, LEDs were built on aluminum heat sinkers. The images were taken in a dark room, where the only sources of light were those designed for this study. Care was taken to position the light sources and the camera so as to minimize the presence of shadows in the images.

For the clinical diagnosis, the study procedure consisted in taking photographs with a DermLite II Hybrid[®] dermatoscope under white light illumination. In addition, images were captured with the digital cameras used in this study under the two light conditions described above.

For each recorded photograph, a lesion area was selected and its RGB histograms were processed, as follows: the total intensity (corresponding to the total number of pixels in the selected area for a given color) was taken as the sum of the areas of all histogram bins. The area of each bin was calculated as the number of pixels in the bin (corresponding to frequency) multiplied by the bin width (corresponding to an intensity range). Subsequently, the intensities of the three RGB histograms were added to obtain the total area intensity. As an example, the user interface developed to process the

recorded digital images of skin lesions is presented in Fig. 1. The left side of the figure displays the lesion area selected from the original digital image presented in the rightmost part of the figure, together with the matching RGB histograms. The digital image corresponds to a foot lesion, clinically diagnosed as an acral nevus, photographed under white light.

For comparison, a region in the same area as the lesion, but of a healthy neighboring zone, was selected from the image (as seen in the central column of Fig. 1). This area was subjected to the same RGB intensity evaluation. Using the healthy perilesional skin intensity as reference, the percentage change in lesion intensity was then evaluated.

In Fig. 1, the total RGB intensities are shown in the lower right corner, while the identification of the patient appears in the upper right corner of the figure.

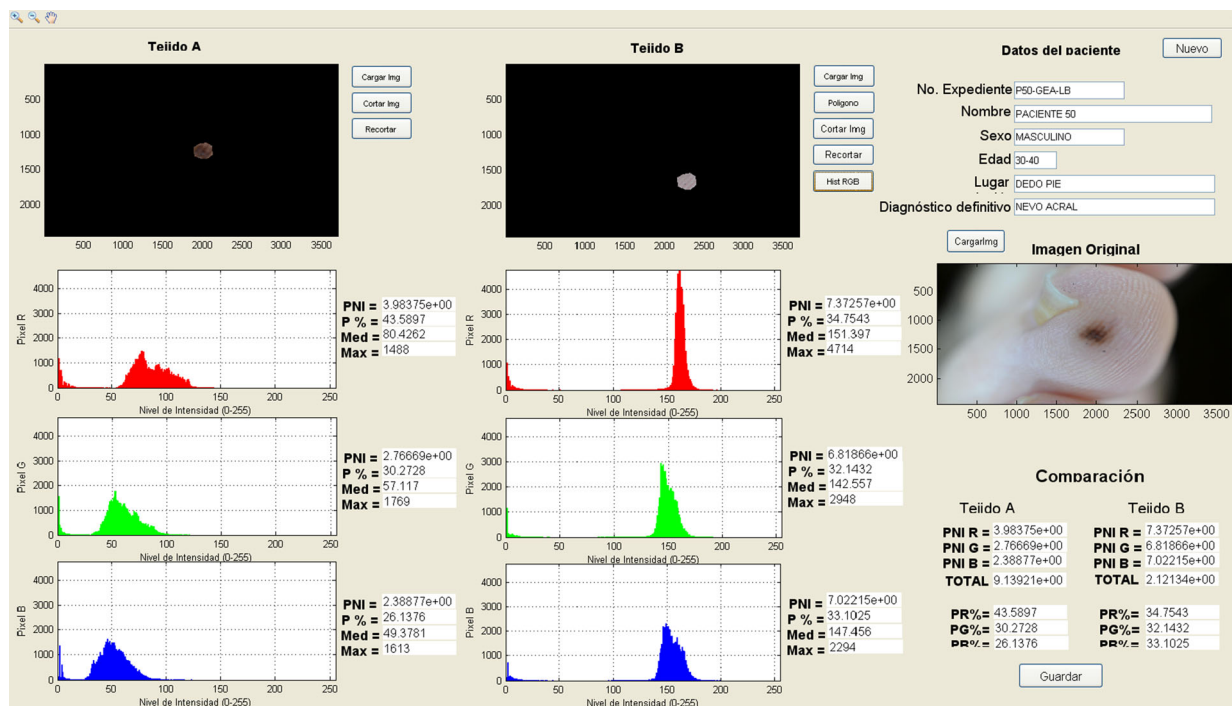


Fig. 1 Processing of the digital image of a toe lesion, taken under white light. Images of the lesion and the perilesional zone, together with their respective RGB histograms, are also shown

Figure 2 shows images and histograms recorded for the same toe lesion as before, but this time using UV illumination.

For spectroscopic measurements, the LEDs (one white or one UV LED) were coupled to the bifurcated optical fiber, and the latter was connected to the spectrometer through a subminiature version A (SMA) connector.

Prior to each set of spectroscopic measurements, the noise spectrum was measured by placing the optical fiber probe on the tissue in the absence of any excitation light. The spectrum thus obtained was then subtracted from every measured spectrum. Spectra were recorded by placing the optical fiber probe on at least three points of the lesion, on the surrounding tissue, and finally on the normal skin of the inner arm, which was chosen as a control because it typically shows uniform optical patterns. The irradiation power of the

light source was set to 1.5 mW, and the spectrometer was configured with a 100-ms integration time. Spectra were smoothed using a fourth-order Savitzky–Golay filter to remove high-frequency noise caused by the spectrometer.

For each patient, a description of the lesions, the clinical and histological diagnosis, the gathered spectra, and the photographs were recorded and entered into a database developed in MATLAB [26].

Skin lesions were organized into six groups according to the histology report: BCC, SCC, melanoma, SK, melanocytic nevi, and other. In addition, the patients were divided into groups by Fitzpatrick skin phototype.

For all analyzed lesions, a corresponding biopsy and histopathology study report was performed, which was used as validation of the optical results of the present study.

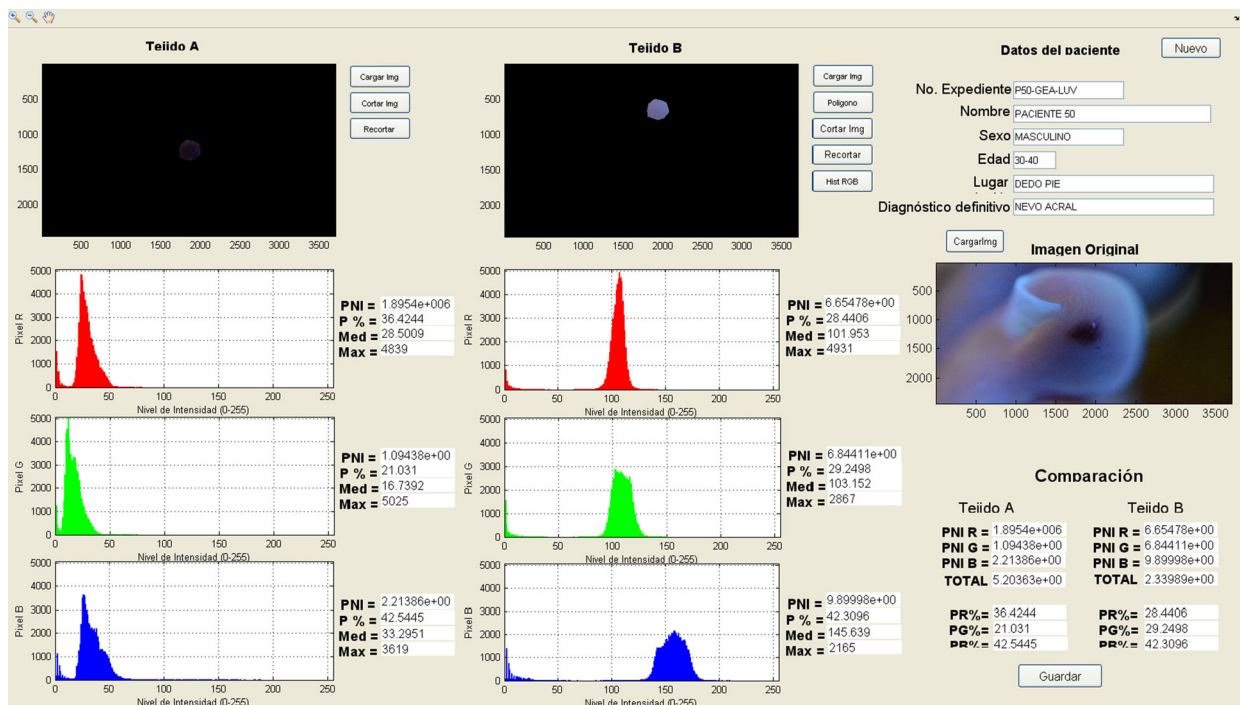


Fig. 2 Processing of digital image of a toe skin lesion under UV light. Images of the lesion and the perilesional zone are also shown, with their respective histograms

Compliance with Ethics Guidelines

All procedures followed were in accordance with the ethical standards of the responsible committee on human experimentation (institutional and national) and with the Helsinki Declaration of 1964, as revised in 2013. Informed consent was obtained from all patients for inclusion in the study.

RESULTS

Fifty patients who were scheduled for biopsy signed the informed consent form and participated in the photography and spectroscopy measurement sessions. From these 50, nine patients were ultimately excluded because their biopsy procedures were cancelled. For one patient, the cancellation occurred due to clinical improvement with medical treatment, and the lesion was found to be inflamed SK, while the remaining eight patients did not attend their biopsy appointments. Thus, data were collected from 41 patients, including 29 women and 12 men. The mean age of the patients was 63.7 years, with a median age of 67 years and standard deviation (SD) of 15.85 years. A total of 50 lesions were analyzed (some patients had more than one lesion). On the Fitzpatrick scale, 20 patients were classified as having skin phototype IV (48.8%), 19 as phototype III (46.3%), one as phototype II (2.4%), and one as phototype V (2.4%). There were no patients with skin phototypes I or VI.

As confirmed by histopathological studies, BCC was the most common lesion, present in 15 of the 41 cases. Of these, nine were pigmented. Melanocytic nevi were the next most common tumor, with 11 cases. These included nine intradermal nevi (IDN), one cellular blue nevus,

and one acral nevus. All nine cases of IDN were pigmented lesions. The other reported skin lesions comprised seven SCC, five melanomas, four SK, one basal squamous carcinoma, one trichofolliculoma, one venous lake, one severe solar elastosis, one lymphocytoma cutis, one sebaceous hyperplasia, one keloid, and one proliferation of atypical melanocytes.

The clinical differential diagnoses of BCC were SK, IDN, sebaceous hyperplasia, SCC, and MM. Some SCCs were diagnosed as hypertrophic AK, irritated SK, or keratoacanthoma. The clinical differential of basal squamous carcinoma and venous lake was BCC. A typical melanocytic proliferation was classified as acral nevus.

Diffuse Reflectance Spectroscopy Under White Light

Because of the large number of lesions investigated, and given the fact that the main interest of the study was centered on pigmented lesions, the following sections will focus primarily on cases related to BCC (9), IDN (10), and melanoma (4) lesions.

Figure 3 shows the diffuse reflectance spectra of the normal cheek and forehead tissues in patients with skin phototypes III and IV. The curves are the average spectra for all sampled patients in each skin phototype group. The vertical bars in the graphics account for the observed standard deviations. It is clear from the figure that there is a distinct difference in the diffuse reflectance spectra of the forehead for the two phototypes.

In Fig. 4A, B, the average diffuse reflectance spectra of pigmented BCC, IDN, and melanoma cutaneous lesions obtained under white LED light are displayed separately for patients with skin phototypes III and IV, respectively. Typical points of hemoglobin absorption at 545 and

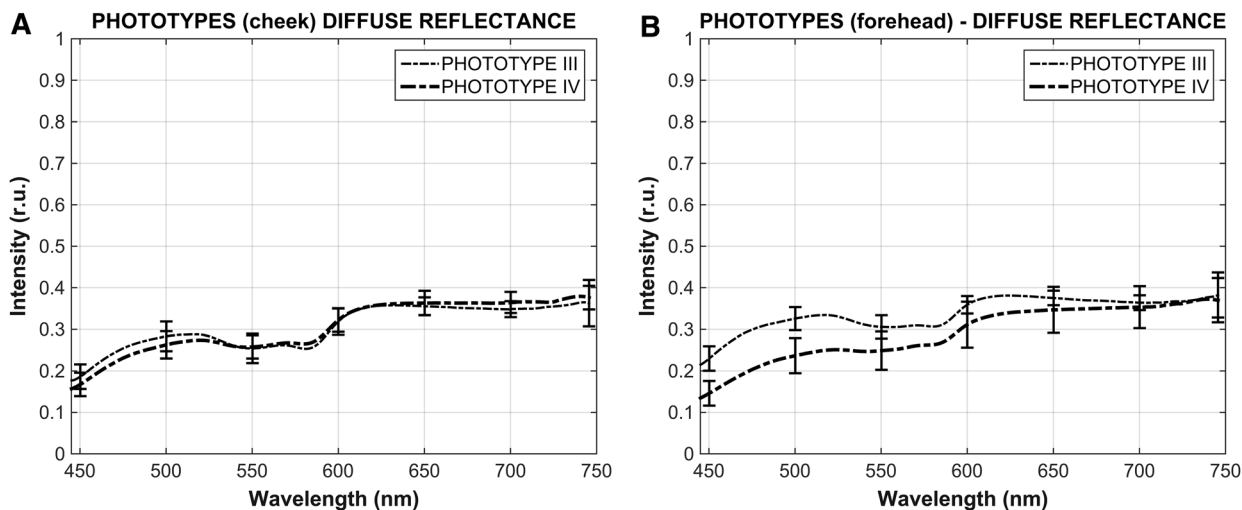


Fig. 3 Cheek (A) and forehead (B) diffuse reflectance spectra for patients with skin phototypes III and IV

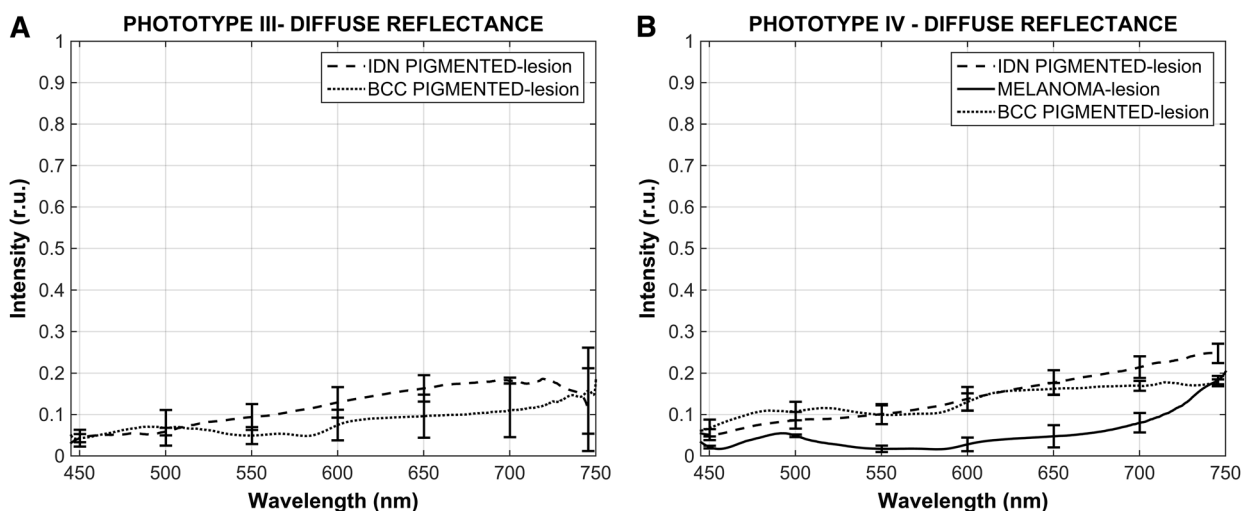


Fig. 4 Diffuse reflectance spectra of cutaneous pigmented IDN, BCC, and melanoma lesions in patients with skin phototypes III (A) and IV (B)

575 nm appear in the diffuse reflectance spectra for all except pigmented IDN. From Fig. 4, it is clear that the spectral shape of each skin lesion is different, irrespective of the phototype. These spectra can be differentiated from one another by their intensity, especially in the range of 550 to 725 nm. It is worth noting that for BCC, the intensity in phototype IV is higher than that in

phototype III, while for IDN the intensities are similar between phototypes.

Of note, the general trend of the curves in Fig. 4 agrees with previous reports by Borisova et al. [27, 28], which showed that the intensity of the reflectance spectra in the region between 550 and 725 nm increased in the order melanoma < BCC < IDN < normal skin.

Spectroscopic Response Under UV Light

The spectral emission of the UV LED used in the study is shown in Fig. 5. A high emission peak is observed extending from 325 to 412 nm, with a maximum at 375 nm instead of 365 nm, as was stated in the LED datasheet supplied by the manufacturer. A soft emission is also present from ~ 410 to 800 nm, with a local maximum at around 500–550 nm, as shown in the inset of

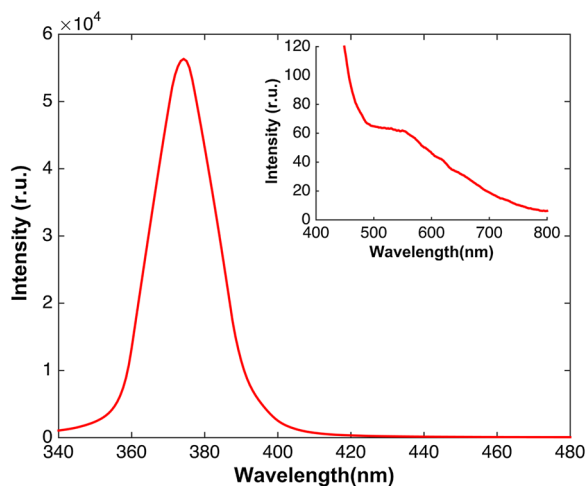


Fig. 5 Measured spectral emission of the NCU033AT ultraviolet LED (Nichia Corp.). The *inset* is a zoom of the right tail of the UV main peak

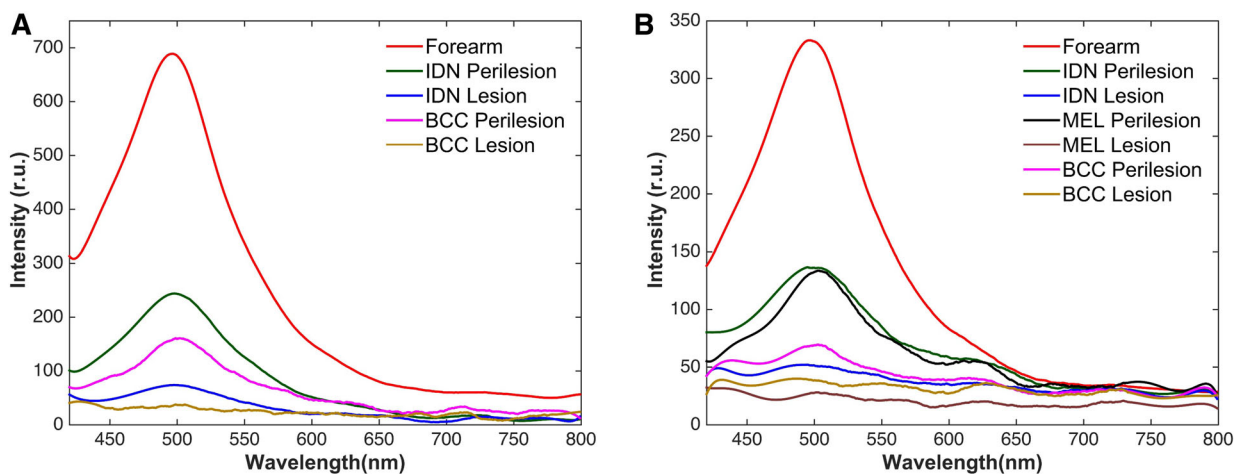


Fig. 6 Measured spectra under UV illumination for pigmented skin lesions in patients with skin phototypes III (A) and IV (B)

Fig. 5, where a zoom image of the appropriate region of the emission spectrum is plotted.

This soft emission was detected in all spectroscopic measurements, overlapping with the possible tissue fluorescence in this same wavelength region, as can be seen in Fig. 6, where the spectra observed for several skin lesions and their surrounding region are displayed separately for patients with skin phototypes III and IV. The assumption of the fluorescence emission in this region is supported by previous reports [28] in which the same fluorescence distinctive mark was used to discriminate between BCC and SCC lesions. Unfortunately, with the UV source used in this work, it was either impossible or very difficult to attempt such differentiation.

For the sake of comparison, the measured average spectra for the forearm region are plotted in Fig. 6. Here, the previously mentioned soft emission peak from the source is seen as a reflection from the normal skin. In the same wavelength region, some fluorescence should be expected [28], but it is difficult to resolve it from the former. In any case, it is evident from Fig. 6 that for the spectra of all studied lesions—identified in the graphics as intradermal nevus

(IDN), basal cell carcinoma (BCC), and melanoma (MEL)—the intensity in the wavelength region around 500 nm is much lower than that in the nearby healthy zone, leading to the conclusion that either the fluorescence is much weaker or the peak intensity of the soft emission is absorbed more strongly in the lesions than in the perilesional zone, or both. This characteristic is common to all lesions, but the differences in the spectra are not sufficient to unequivocally differentiate one lesion from another, nor are there clear differences between the spectra of the lesions in the region of larger wavelengths, between 575 and 800 nm.

This analysis leads us to conclude that UV spectroscopy performed with the UV source

described above is not an effective tool for the differential diagnosis of IDN, BCC, or melanoma. However, the distinct absorption of the lesions in comparison to the neighboring healthy skin tissue points to the possibility of obtaining high-contrast images using this particular UV LED.

Such result was confirmed for the lesion images obtained under UV light, where the lesion edges were identified more precisely than in the photos taken under white light, even for non-pigmented lesions.

As an example, in Fig. 7A, B, photographs taken under white and UV light from a non-pigmented BCC in the nose are presented, together with the UV spectra measured in one point in the perilesional region and five points

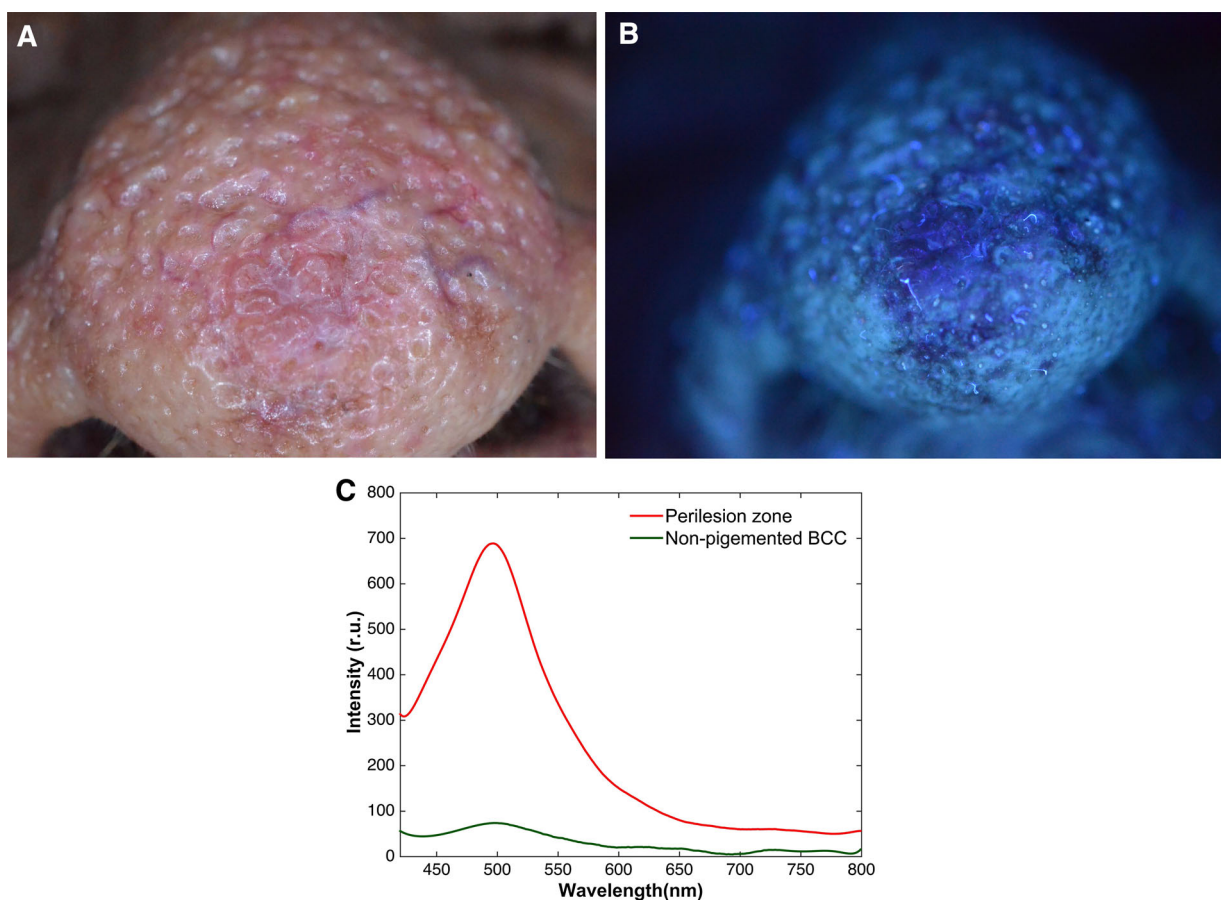


Fig. 7 Digital images of a non-pigmented BCC taken under white LED light (A) and UV light (B). C Spectra measured on the lesion and on the perilesional skin using the UV light source

on the tumor. The displayed BCC spectrum is the average of the five measured curves. In the UV image, the lesion is evident, with well-defined edges, whereas these are hardly seen in the white light photograph. In the measured BCC spectrum in Fig. 7C, the previously mentioned absorption in the region from 425 to 600 nm is evident.

UV and White Light Images

From the recorded images, it was necessary to exclude lesions that were in hairy regions, due to the technical difficulties encountered for image analysis. In addition, one case of SCC

was excluded because of significant bleeding, which made it impossible to take an appropriate photograph. One other case was excluded due to poor image quality. Thus, a total of 39 lesions were ultimately considered.

Figure 8 shows some examples of the obtained images. Figure 8A, B shows photographs of a diagnosed melanoma taken under white and UV light, respectively. Figure 8C displays a BCC recorded under white illumination, while Fig. 8D depicts the same lesion, but photographed using UV light. As stated above, lesion details that were not easily seen in white light images were able to be detected in UV images.

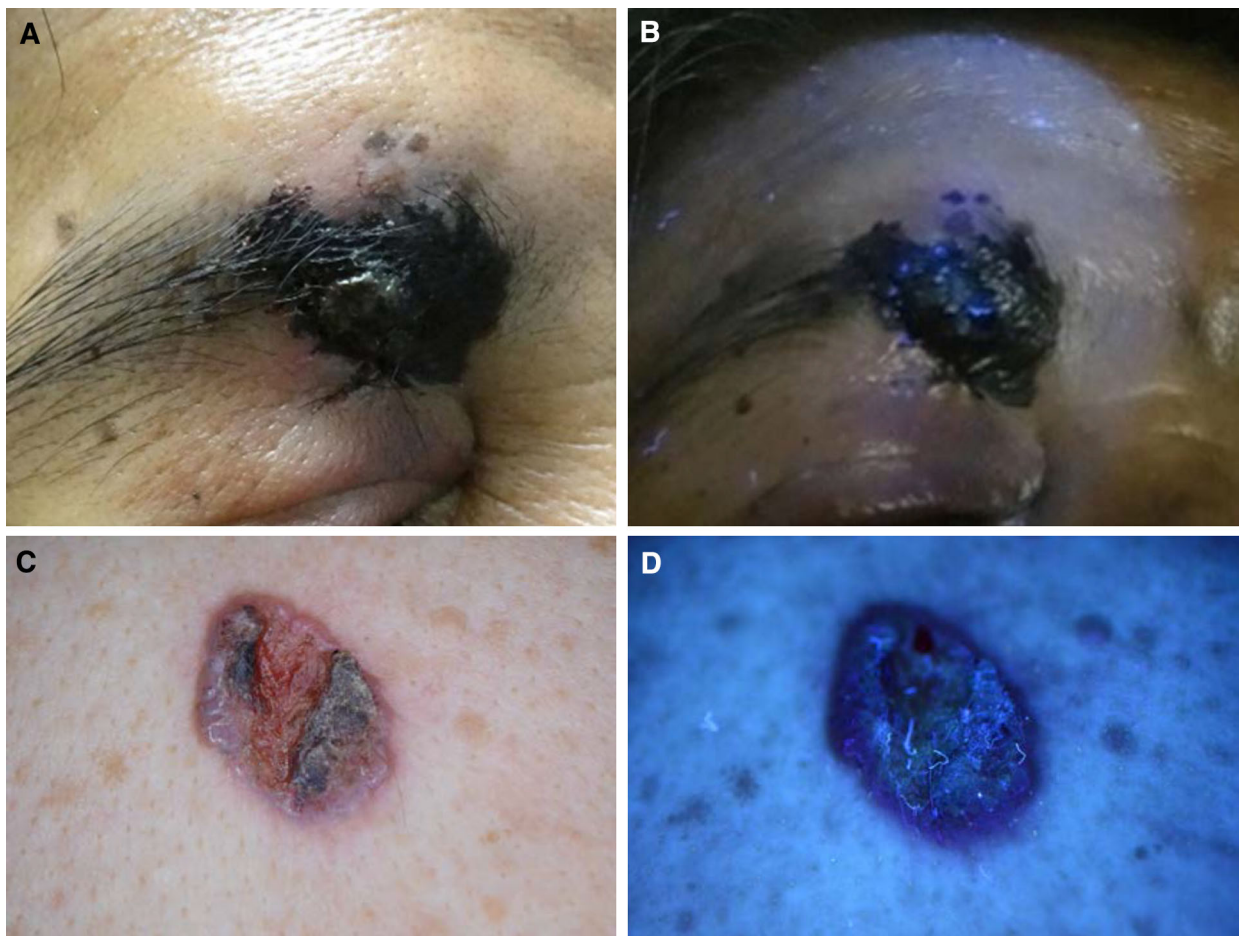


Fig. 8 Images of some of the examined skin lesions. Melanoma under white light (**A**) and under UV illumination (**B**). BCC under white (**C**) and UV (**D**) light

Table 1 Percentage change in total intensity (measured from digital image RGB histograms) of lesions in patients with skin phototype IV, relative to the intensity of perilesional healthy tissue

Skin lesion	Intensity change under white light (%)	Intensity change under UV light (%)
Melanoma	−88 to −62	−78 to −67
Pigmented IDN	−61 to −25	−74 to −32
Non-pigmented IDN (one patient)	−15	−4
Pigmented BCC	−70 to −34	−57 to −34
SCC	−23 to −5	7 to 446

It must be noted that artifacts were present in several UV images, as in the case of Fig. 8D, where fiber scraps, presumably from the gauze used to clean the lesion, are clearly observed. Such fibers could also come from clothing or other objects used by patients, and this should be taken into account in future studies.

All images were subjected to intensity analysis. Table 1 shows the variation among lesions in terms of percentage change in intensity relative to healthy tissue in patients with skin phototype IV. With the exception of SCC under UV light, the light intensity from the lesions was lower than that from healthy tissue, which shows that the percentage intervals for white light can differentiate melanoma from melanocytic nevi and SCC. Under UV light, the intensity was able to differentiate melanoma from pigmented BCC and SCC, but not from pigmented melanocytic nevi. In addition, SCC was able to be differentiated from all other lesions under UV light. This was not observed under white light, where there were no differences between SCC and non-pigmented melanocytic nevi.

Table 2 shows the variation among lesions in terms of percentage change in intensity relative to healthy perilesional tissue in patients with skin phototype III. The data here show that under both white and UV light, only SCC was able to be differentiated from the other studied lesions. Pigmented melanocytic nevi and

pigmented BCC were differentiated to a lesser extent, due to the overlapping of intervals. Unfortunately, we did not obtain any information about melanoma in this skin type, in which a lower range of variation would be expected in comparison to skin phototype IV.

One melanoma occurred in a patient with skin phototype V, as shown in Table 3. In this case, the difference in light intensity was lower than that in patients with skin type IV, which can be explained if we consider that skin phototype V represents a darker skin color, so the difference in light intensity between the lesion and perilesional tissue is smaller.

Finally, one skin phototype II patient with BCC diagnosis showed poor pigmentation in the lesion, which made it scarcely visible. However, sporadic small dark spots were detected in the area of the lesion. The intensity change values are reported in Table 4.

A more statistically formal test was performed to determine whether the analyzed skin lesions could be differentiated using the recorded digital images and their RGB intensity histograms. For this, the ratio of the total area intensity of the lesion in the image to the total intensity of a nearby region of healthy tissue of the same area was calculated, and the values of such ratios were grouped according to lesion type, separately for phototypes III and IV.

Table 2 Percentage change in total intensity between lesions and perilesional tissue in patients with skin phototype III

Skin lesion	Intensity change under white light (%)	Intensity change under UV light (%)
Pigmented IDN	−57 to −45	−78 to −52
Pigmented BCC	−55 to −10	−56 to −28
Non-pigmented BCC	−24 to −4	−57 to −17
SCC	9 to 48	53 to 157
SCC in situ	−44 to 3	−39 to 52

Table 3 Percentage change in total intensity in melanoma (one patient with skin phototype V)

Patient number	Intensity change under white light (%)	Intensity change under UV light (%)
20	−46	−38

Table 4 Percentage change in total intensity in BCC (one patient with skin phototype II)

Patient number	Intensity change under white light (%)	Intensity change under UV light (%)
14	−11	−65

In Figs. 9 and 10, the mean values of the intensity ratio for each group are plotted, together with a bar indicating the corresponding standard deviation (SD).

Figure 9 shows the intensities gathered from images taken for phototype III patients, while Fig. 10 presents the intensity relations in images taken in phototype IV patients. In both figures, graphic A corresponds to images taken under white light, and graphic B matches UV images.

The aforementioned observation of lower intensity in the lesion than in the surrounding healthy tissue—i.e. intensity ratio of less than 1.0—can be observed in Figs. 9 and 10 for all analyzed lesion groups except for SCC under UV light in phototype IV and with both types of illumination in phototype III.

The intensity ratio samples were analyzed using one-way analysis of variance (ANOVA) to check the null hypothesis that the samples being compared have the same mean statistically, or equivalently, to check whether

the samples come from the same population. An ANOVA *p* value less than 0.05 indicates that the null hypothesis must be rejected with a 95% significance level, thus indicating that the samples come from different populations. In other words, an ANOVA *p* value lower than 0.05 would indicate that the lesions of the different groups can be differentiated from one another using the digital image intensity ratios between the lesion and its surrounding healthy region as the analysis variable.

In Figs. 9 and 10, the letters next to each lesion-type SD bar indicate the kinds of lesions that can be discriminated from the lesion in question, following the scheme described in the figure captions. Looking at these letters, it becomes evident that the conclusions drawn from Tables 1 and 2 are confirmed.

In patients with skin phototype III (Fig. 9), IDC can be discriminated from all other lesions under both white and UV light; the same statement is valid for SCC under white light,

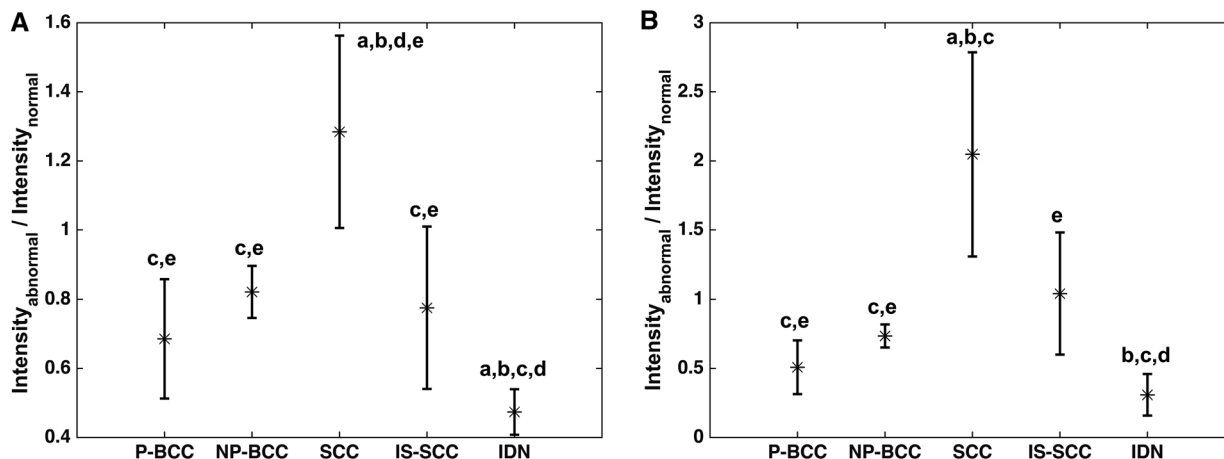


Fig. 9 Total intensity ratios of digital images taken in patients with skin phototype III under white light (A) and UV light (B). *P-BCC* pigmented basal cell carcinoma, *NP-BCC* non-pigmented basal cell carcinoma, *SCC* squamous cell carcinoma, *IS-SCC* in situ squamous cell

carcinoma, *IDN* intradermal nevus. *a* $p < 0.05$, compared to P-BCC; *b* $p < 0.05$, compared to NP-BCC; *c* $p < 0.05$, compared to SCC; *d* $p < 0.05$, compared to IS-SCC; *e* $p < 0.05$, compared to IDN

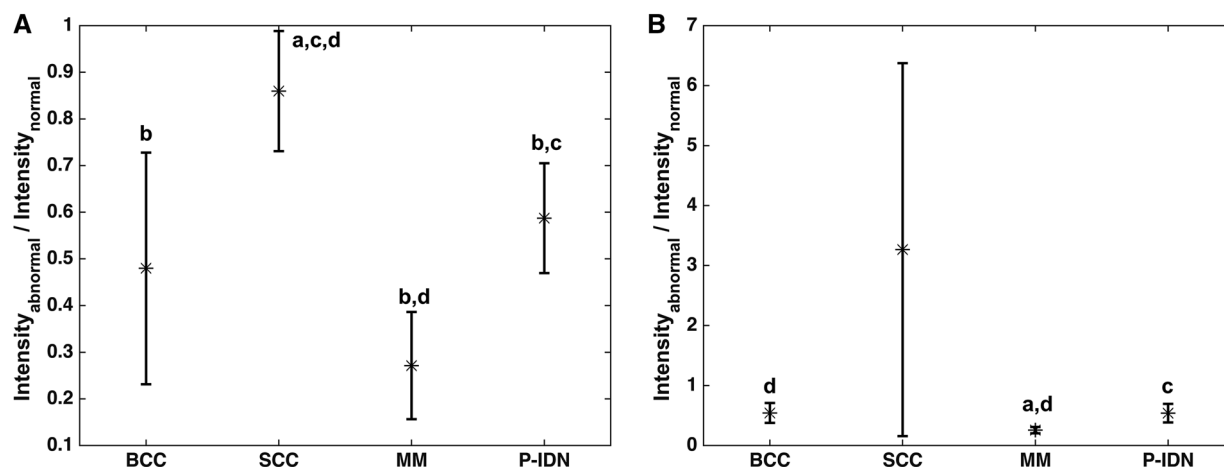


Fig. 10 Total intensity ratios of digital images in patients with skin phototype IV, recorded under white (A) and UV (B) light. *BCC* basal cell carcinoma, *SCC* squamous cell carcinoma, *MM* malignant melanoma, *IDN* intradermal

nevus. *a* $p < 0.05$, compared to BCC; *b* $p < 0.05$, compared to SCC; *c* $p < 0.05$, compared to MM; *d* $p < 0.05$, compared to IDN

whereas under UV illumination, SCC can be differentiated from BCC (pigmented and non-pigmented) and from IDN, but not from in situ SCC. On the other hand, Fig. 9 shows that pigmented and non-pigmented BCC cannot be discriminated using the proposed method, regardless of the illumination type.

For phototype IV, shown in Fig. 10, the method allows differentiation of melanoma from SCC and IDN under white light, and from BCC and SCC under UV light. For its part, SCC can be differentiated from all other lesions under white light but not under UV light.

DISCUSSION

Several research groups have studied the use of fluorescence for the detection and differentiation of skin cancer [19, 27–30]. Diffuse reflectance spectroscopy has also been used to study cutaneous malignancies; Borisova et al. [28] reported spectra for BCC and melanoma lesions similar to those shown in Fig. 4 of this paper. Cordo et al. [31] applied diffuse reflectance spectroscopy from 550 to 1000 nm in healthy skin (inner and outer forearm), in addition to different pigmented skin lesions and their adjacent areas. The authors found that the major differences were in the wavelength of maximum reflectance and in the slope of the spectral curves in the wavelength interval between 760 and 910 nm.

The principal contribution of the present study is the application of UV and white light LEDs to obtain color images whose histograms help to differentiate skin tumors. Although multispectral images at different spectral bands in the visible region of the electromagnetic spectrum [32] and at 360 nm in the UV range [33] have been used for melanoma diagnosis, as well as white light digital image processing for differentiation of melanoma and non-melanoma skin lesions [34–36], to our knowledge, this is the first time that digital image intensity RGB histograms have been successfully used for the evaluation and discrimination of skin cancer lesions.

With the exception of SCC, in all analyzed cases the intensity of the reflectance shown in the spectra and in the image RGB histograms was higher for the healthy tissue than for the lesions. An important finding was that the results varied according to patient skin phototype. In addition, lower intensity was observed for pigmented versus non-pigmented lesions, and the reflected intensity of melanoma

was lower than that of the other lesions. Although we examined only a small number of lesions, this study produced important data to consider for subsequent studies.

The results for images recorded under white light revealed a difference between melanoma and melanocytic nevi. In addition, in the images taken under UV light at 375 nm, it was possible to differentiate between melanoma and pigmented BCC. We propose this method as an auxiliary diagnostic tool, prior to biopsy, for distinguishing among these pigmented entities. However, we did not find patterns in this study to support differentiation between BCC and pigmented melanocytic nevi, and we suggest that further studies are needed.

An advantage of the imaging study is that the area for analysis can be chosen with great precision. There is no influence of pressure on the tissue, and different areas (lesion, perilesional, and apparently healthy skin) can be compared under the same light. This could help in identifying lesions that are invisible to the naked eye, and in guiding the clinician's choice of biopsy site, especially when using images of the same region obtained with the two different light sources. This finding is in accordance with the recently published study by Nguyen et al. [32, 37] regarding the use of intraoperative artificial fluorescent markers ("fluorescence-guided surgery") to support the delineation of tumor margins.

One drawback that became apparent in the analysis of fluorescence images was that the use of socks, cotton, or bandages could leave protruding millimeter fibers in the UV image; this fact should be taken into consideration in future studies. In addition, larger tumors and those in areas with hair presented difficulties in obtaining pictures and performing intensity measurements.

CONCLUSION

In this study, we found that the diffuse reflectance spectra of pigmented BCC, IDN, and melanoma cutaneous lesions in patients with skin phototypes III and IV were useful in differentiating between these lesions. White light images could thus serve as an auxiliary tool for clinically differentiating between BCC, IDN, and melanoma cutaneous lesions in these patients. The UV light images at 375 nm were able to differentiate melanoma from pigmented BCC.

The results from this pilot study may pave the way for further research to document the value of these new tools in the clinical diagnosis of melanoma and non-melanoma skin cancer. These methods are noninvasive, affordable, and easy to use, and thus could be useful in skin cancer treatment centers.

ACKNOWLEDGEMENTS

No funding or sponsorship was received for this study or publication of this article. All named authors meet the International Committee of Medical Journal Editors (ICMJE) criteria for authorship for this manuscript, take responsibility for the integrity of the work as a whole, and have given final approval for the version to be published.

Disclosures. Stefanie Arroyo-Camarena, Judith Domínguez-Cherit, Lorena Lammoglia-Ordiales, Diego A. Fabila-Bustos, Abraham Escobar-Pio, Suren Stolik, Alma Valor-Reed, and José de la Rosa-Vázquez have nothing to disclose.

Compliance with Ethics Guidelines. All procedures followed were in accordance with

the ethical standards of the responsible committee on human experimentation (institutional and national) and with the Helsinki Declaration of 1964, as revised in 2013. Informed consent was obtained from all patients for inclusion in the study.

Open Access. This article is distributed under the terms of the Creative Commons Attribution-NonCommercial 4.0 International License (<http://creativecommons.org/licenses/by-nc/4.0/>), which permits any noncommercial use, distribution, and reproduction in any medium, provided you give appropriate credit to the original author(s) and the source, provide a link to the Creative Commons license, and indicate if changes were made.

REFERENCES

1. Díaz González JM, Peniche Castellanos A, Fierro Arias JM, Ponce Olivera RM. Cáncer de piel en pacientes menores de 40 años. Experiencia de cuatro años en el Hospital General de México. *Gac Méd Méx.* 2011;147:17–21.
2. Gutierrez RM. Cáncer de piel. *Rev Fac Med UNAM.* 2003;46(4):166–71.
3. De Leeuw J, van der Beek N, Neugebauer WD, Bjerring P, Neumann M. Fluorescence detection and diagnosis of non-melanoma skin cancer at an early stage. *Lasers Surg Med.* 2009;41:96–103.
4. Jurado-Santa Cruz F, Medina-Bojórquez A, Gutiérrez-Vidrio RM, Ruiz-Rosillo JM. Prevalencia del cáncer de piel en tres ciudades de México. *Rev Med Ins Mex Seguro Soc.* 2011;49(3):253–8.
5. Dourmishev L, Rusinova D, Botev I. Clinical variants, stages, and management of basal cell carcinoma. *Indian Dermatol Online J.* 2013;4(1):12–7.
6. Nuño-González A, Vicente-Martín F, Pinedo-Moraleda F, López-Estebanza J. Carcinoma epidermoide cutáneo de alto riesgo. *Actas Dermosifiliogr.* 2012;103:567–78.
7. Reyes G, Romero A, Alcántara P, Mata M, Parraguire S, Vega-Memije E. Caracterización epidemiológica y

- concordancia clínico-patológica del cáncer de piel en el Hospital General Dr. Manuel Gea González. *Dermatol Cosmét Méd Quir.* 2007;5:80–7.
8. Gloster H, Neal K. Skin cancer in skin of color. *J Am Acad Dermatol.* 2006;55:741–60.
 9. Káram-Orantes M, Toussaint-Caire S, Domínguez-Cherit J, Vega-Memije E. Características clínicas e histológicas del melanoma maligno en el Hospital General “Dr. Manuel Gea González”. *Gac Med Mex.* 2008;144(3):219–23.
 10. Ruiz AB, Quiñones R, Domínguez AE. Dermatoscopia de las queratosis seborreicas y sus diferentes caras. *Dermatol Rev Mex.* 2012;56(3):193–200.
 11. Senel E. Dermatoscopy of non-melanocytic skin tumors. *Indian J Dermatol Venereol Leprol.* 2011;77:16–22.
 12. Braun RP, Rabinovitz H, Oliviero M, Kopf A, Saurat JH. Dermoscopy of pigmented skin lesions. *J Am Acad Dermatol.* 2005;52:109–21.
 13. Marchesini R, Bono A, Bartoli C, Lualdi M, Tomatis S, Cascinelli N. Optical imaging and automated melanoma detection: questions and answers. *Melanoma Res.* 2002;12:279–86.
 14. Markovic S, Erickson L, Rao R, et al. Malignant melanoma in the 21st century, Part 1: epidemiology, risk factors, screening, prevention, and diagnosis. *Mayo Clin Proc.* 2007;82(3):364–80.
 15. Salerni E. Uso de la microscopia confocal de reflectancia en dermatología. *Dermatol Argent.* 2011;17(3):230–5.
 16. Ulrich M, Lange-Asschenfeldt S. In vivo confocal microscopy in dermatology: from research to clinical application. *J Biomed Opt.* 2013;18(6):061212-1–9.
 17. Nehal KS, Gareau D, Rajadhyaksha M. Skin imaging with reflectance confocal microscopy. *Semin Cutan Med Surg.* 2008;27:37–43.
 18. Wagnieres G, Star W, Wilson B. In vivo fluorescence spectroscopy and imaging for oncological applications. *Photochem Photobiol.* 1998;68:603–32.
 19. Liu Q. Role of optical spectroscopy using endogenous contrasts in clinical cancer diagnosis. *World J Clin Oncol.* 2011;10:50–63.
 20. Groce C, Fiorani S, Locatelli D, Nano R, Ceroni M, Tancioni F, Giombelli E, Benericetti E, Bottiroli G. Diagnostic potential of autofluorescence for and assisted intraoperative delineation of glioblastoma resections margins. *Photochem Photobiol.* 2003;77:309–18.
 21. Breslin T, Xu F, Palmer G, Zhu C, Gilchrist K, Ramanujam N. Autofluorescence and diffuse reflectance properties of malignant and benign breast tissues. *Ann Surg Oncol.* 2003;11:65–70.
 22. Huang Z, Zheng W, Xie S, Chen R, Zeng H, Mclean D, Lui H. Laser-induced autofluorescence microscopy of normal and tumor human colonic tissue. *Int J Oncol.* 2004;24:59–63.
 23. Mirabal Y, Chang S, Atkinson E, Malpica A, Follen M, Richards-Kortum R. Reflectance spectroscopy for in vivo detection of cervical precancer. *J Biomed Opt.* 2002;7:587–94.
 24. Panjephour M, Julius C, Phan M, Vo-Dinh T, Overholt S. Laser-induced fluorescence spectroscopy for in vivo diagnosis of non-melanoma skin cancers. *Laser Surg Med.* 2002;31:367–73.
 25. Wang S, Zhao J, Lui H, et al. In vivo near-infrared autofluorescence imaging of pigmented skin lesions: methods, technical improvements and preliminary clinical results. *Skin Res Technol.* 2013;19:20–6.
 26. MATLAB. The mathworks Inc. Massachusetts: Natick; 2012.
 27. Borisova E, Pavlova P, Pavlova E, Troyanova P, Avramov L. Optical biopsy of human skin—a tool for cutaneous tumor’s diagnosis. *Int J Bioautomation.* 2012;16:53–72.
 28. Borisova E, Pavlova E, Troyanova Petranka, Zhelyazkova A, Genova T, Avramov L. Using spectroscopy to diagnose skin cancer. *SPIE Newsroom.* doi:10.1117/2.1201405.005509.
 29. Rajaram N, Kovacic D, Migden M, Reichenberg J, Nguyen T, Tunnell J. In vivo determination of optical properties and fluorophore characteristics of non-melanoma skin cancer. *Proc SPIE.* 2009;7161:716102–9.
 30. Brancalion L, Durkin A, Tu J, Menaker G, Fallon J, Kollias N. In vivo fluorescence spectroscopy of nonmelanoma skin cancer. *Photochem Photobiol.* 2001;73:178–83.
 31. Cordo M, Sendra J, Viera A, Santana A, López Silva M. Diferenciación de piel sana y lesiones cutáneas pigmentadas mediante espectroscopía de reflectancia óptica difusa. *Opt Pura Apl.* 2006;39(4):341–54.
 32. Wang SQ, Ravinovitz H, Oliviero M. Computer aided diagnosis for cutaneous melanoma. In: Rigel

- DS, Friedman RJ, Dzubow LM, Reintgen DS, Bystryn J-C, Marks R, editors. *Cancer of the Skin*. Elsevier Saunders; 2005. p. 449–55.
33. Gamble RG, Asdigian NL, Aalborg J, Gonzalez V, Box NF, Huff LS, Barón AE, Morelli JG, Mokrohisky ST, Crane LA, Dellavalle RP. Sun damage in ultraviolet photographs correlates with phenotypic melanoma risk factors in 12-year-old children. *J Am Acad Dermatol*. 2012;67(4):587–97.
 34. Chang W-Y, Huang A, Yang C-Y, Lee C-H, Chen Y-C, Wu T-Y, Chen GS. Computer-aided diagnosis of skin lesions using conventional digital photography: a reliability and feasibility study. *PLoS One*. 2013;8(11):e76212.
 35. Jaworek-Korjakowska J. Computer-aided diagnosis of micro-malignant melanoma lesions applying support vector machines. *Biomed Res Int*. 2016;2016:4381972.
 36. Burrioni M, Corona R, Dell'Eva G, Sera F, Bono R, Puddu P, Perotti R, Nobile F, Andreassi L, Rubegni P. Melanoma computer-aided diagnosis: reliability and feasibility study. *Clin Cancer Res*. 2004;10:1881–6.
 37. Nguyen QT, Tsien RY. Fluorescence-guided surgery with live molecular navigation—a new cutting edge. *Nat Rev Cancer*. 2013;13:653–62.